Supplementary Materials

Table S1 Bond lengths of optimized favipiravir and Fav+$XTiO_4H_2$ at gas and water solvent calculated at B3LYP/LANL2DZ basis set.

Bond length (Å)	Favipiravir		Fav+$Ti_2O_4H_2$		Fav+$PtTiO_4H_2$		Fav+$ZrTiO_4H_2$		Fav+$ZnTiO_4H_2$	
	Gas	Water	Gas	Water	Gas	Water	Gas	Water	Gas	Water
F1-C10	1.391	1.394	1.399	1.412	1.384	1.383	1.401	1.425	1.382	1.384
O2-C8	1.246	1.258	1.341	1.334	1.272	1.284	1.352	1.332	1.269	1.279
O3-C11	1.254	1.265	1.365	1.363	1.280	1.288	1.377	1.370	1.275	1.281
N4-C8	1.438	1.424	1.347	1.346	1.404	1.395	1.344	1.347	1.405	1.397
N4-C9	1.372	1.364	1.406	1.412	1.377	1.359	1.411	1.439	1.376	1.361
N4-H12	1.018	1.020	1.017	1.018	1.019	1.022	1.017	1.016	1.020	1.022
N5-C7	1.330	1.336	1.429	1.429	1.343	1.340	1.440	1.446	1.342	1.338
N5-C10	1.346	1.337	1.309	1.317	1.343	1.330	1.308	1.325	1.341	1.332
N6-C11	1.375	1.365	1.373	1.377	1.357	1.342	1.376	1.380	1.350	1.342
N6-H14	1.011	1.012	1.008	1.009	1.012	1.014	1.008	1.009	1.013	1.014
N6-H15	1.012	1.013	1.012	1.012	1.013	1.015	1.012	1.011	1.014	1.015
C7-C8	1.488	1.477	1.448	1.451	1.463	1.453	1.449	1.447	1.460	1.456
C7-C11	1.515	1.511	1.396	1.396	1.484	1.494	1.394	1.391	1.493	1.499
C9-C10	1.374	1.380	1.406	1.393	1.380	1.389	1.406	1.384	1.383	1.388
C9-H13	1.083	1.082	1.077	1.077	1.082	1.081	1.077	1.077	1.082	1.082

Table S2 Bond angles of optimized Favipiravir and Fav+$XTiO_4H_2$ at gas and water solvent calculated at B3LYP/LANL2DZ basis set.

Bond Angle (º)	Favipiravir		Fav+$Ti_2O_4H_2$		Fav+$PtTiO_4H_2$		Fav+$ZrTiO_4H_2$		Fav+$ZnTiO_4H_2$	
	Gas	Water	Gas	Water	Gas	Water	Gas	Water	Gas	Water
C8-N4-C9	125.667	125.667	123.472	123.243	124.649	124.649	122.853	122.853	124.777	124.777
C8-N4-H12	115.116	115.116	116.861	117.752	115.845	115.845	117.905	117.905	115.912	115.912
C9-N4-H12	119.218	119.218	119.666	119.005	119.506	119.506	119.242	119.242	119.310	119.310
C7-N5-C10	121.334	121.334	116.764	116.061	120.704	120.704	114.710	114.710	120.446	120.446
C11-N6-H14	119.492	119.492	120.544	120.714	120.122	120.122	120.771	120.771	120.110	120.110
C11-N6-H15	120.474	120.474	117.575	118.442	120.078	120.078	117.906	117.906	120.278	120.278
H14-N6-H15	120.034	120.034	121.880	120.740	119.800	119.800	121.307	121.307	119.611	119.611
N5-C7-C8	121.545	121.545	119.568	119.711	121.038	121.038	120.422	120.422	121.645	121.645
N5-C7-C11	116.497	116.497	117.962	118.492	116.542	116.542	117.867	117.867	117.317	117.317
C8-C7-C11	121.957	121.957	122.469	121.796	122.421	122.421	121.706	121.706	121.038	121.038
O2-C8-N4	119.039	119.039	117.527	118.166	117.016	117.016	118.174	118.174	118.492	118.492
O2-C8-C7	128.935	128.935	124.113	123.388	128.757	128.757	123.270	123.270	127.867	127.867
N4-C8-C7	112.027	112.027	118.359	118.446	114.228	114.228	118.555	118.555	113.641	113.641
N4-C9-C10	116.262	116.262	114.383	114.321	116.344	116.344	113.874	113.874	116.461	116.461
N4-C9-H13	119.423	119.423	119.721	119.147	119.262	119.262	118.881	118.881	119.217	119.217
C10-C9-H13	124.315	124.315	125.895	126.530	124.395	124.395	127.243	127.243	124.321	124.321

Bond Angle (°)	Favipiravir		Fav+$Ti_2O_4H_2$		Fav+$PtTiO_4H_2$		Fav+$ZrTiO_4H_2$		Fav+$ZnTiO_4H_2$	
	Gas	Water	Gas	Water	Gas	Water	Gas	Water	Gas	Water
F1-C10-N5	116.822	116.822	116.825	115.600	117.296	117.296	114.637	114.637	117.216	117.216
F1-C10-C9	120.013	120.013	115.723	116.191	119.668	119.668	115.872	115.872	119.757	119.757
N5-C10-C9	123.165	123.165	127.451	128.208	123.036	123.036	129.490	129.490	123.027	123.027
O3-C11-N6	122.992	122.992	117.593	116.981	120.328	120.328	115.990	115.990	122.217	122.217
O3-C11-C7	123.032	123.032	121.172	121.354	123.478	123.478	123.326	123.326	121.702	121.702
N6-C11-C7	113.976	113.976	121.234	121.664	116.194	116.194	120.685	120.685	116.081	116.081

Table S3 Dihedral angles of optimized favipiravir and Fav+ $XTiO_4H_2$ at gas and water solvent calculated at B3LYP/LANL2DZ basis set.

Dihedral angle (°)	Favipiravir		Fav+$Ti_2O_4H_2$		Fav+$PtTiO_4H_2$		Fav+$ZrTiO_4H_2$		Fav+$ZnTiO_4H_2$	
	Gas	Water	Gas	water	Gas	Water	Gas	Water	Gas	Water
C9-N4-C8-O2	-179.996	-180.007	179.997	-179.529	-180.000	179.575	-180.000	-179.727	-179.999	179.414
C9-N4-C8-C7	0.007	-0.005	-0.001	0.256	0.000	-0.347	0.000	-0.087	0.000	-0.586
H12-N4-C8-O2	0.001	-0.001	0.000	0.232	0.000	-0.330	0.000	0.067	0.002	-0.282
H12-N4-C8-C7	-179.997	-179.999	-179.998	-179.983	180.000	179.749	180.000	179.707	-179.999	179.718
C8-N4-C9-C10	-0.004	-0.002	0.004	0.465	0.000	0.043	-0.001	1.878	0.000	0.352
C8-N4-C9-H13	179.998	-179.996	179.985	-179.824	-180.000	-179.982	180.000	-178.693	-179.999	-179.689
H12-N4-C9-C10	-180.000	-180.008	-179.999	-179.292	-180.000	179.944	179.999	-177.913	179.999	-179.962
C10-N5-C7-C8	-0.001	-0.011	0.004	0.951	0.001	-0.249	-0.001	3.406	0.001	0.065
C10-N5-C7-C11	-180.004	-180.006	-179.998	-179.337	-179.998	179.619	180.000	-177.435	-179.999	-179.929
C7-N5-C10-F1	-179.997	180.006	-179.998	179.840	180.000	179.972	-180.000	178.594	180.000	179.739
C7-N5-C10-C9	0.004	0.004	-0.001	-0.188	0.001	-0.094	0.000	-1.559	0.000	-0.346
H14-N6-C11-O3	0.003	-0.002	0.009	2.539	-0.001	-0.204	-0.004	-1.522	-0.002	-0.116
H14-N6-C11-C7	-179.997	179.997	-179.932	-177.662	180.000	179.962	-180.003	178.502	179.999	179.832
H15-N6-C11-O3	179.986	-179.989	180.000	178.884	-180.000	179.720	180.006	179.947	-179.999	-179.835
H15-N6-C11-C7	-0.014	0.009	-0.002	-1.318	0.002	-0.113	0.001	-0.030	0.001	0.112
N5-C7-C8-O2	179.998	180.014	179.999	178.778	180.000	-179.462	-179.999	176.934	179.999	-179.630
N5-C7-C8-N4	-0.004	0.012	-0.002	-0.996	-0.003	0.448	0.001	-2.686	-0.001	0.370
C11-C7-C8-O2	0.002	0.008	0.002	-0.925	-0.001	0.678	0.000	-2.192	-0.001	0.363
C11-C7-C8-N4	179.999	180.006	179.999	179.302	179.996	-179.412	-180.000	178.187	179.999	-179.637
N5-C7-C11-N6	0.023	-0.016	0.003	-0.089	-0.005	0.954	-0.001	-0.806	0.000	-1.661
C8-C7-C11-O3	0.019	-0.012	-0.001	-0.954	-0.003	0.993	0.000	-1.633	-0.003	-1.706
C8-C7-C11-N6	180.020	179.990	-179.998	179.617	179.996	-179.180	-180.000	178.342	179.997	178.346
N4-C9-C10-F1	180.000	180.001	179.994	179.453	180.000	-179.866	-179.999	178.833	180.000	-179.939
N4-C9-C10-N5	-0.002	0.003	-0.003	-0.519	-0.001	0.200	0.001	-1.013	-0.001	0.147
H13-C9-C10-F1	-0.003	-0.006	0.014	-0.233	-0.001	0.160	0.000	-0.539	-0.001	0.104
H13-C9-C10-N5	179.996	179.997	-179.982	179.796	179.998	-179.773	-180.000	179.616	179.999	-179.810

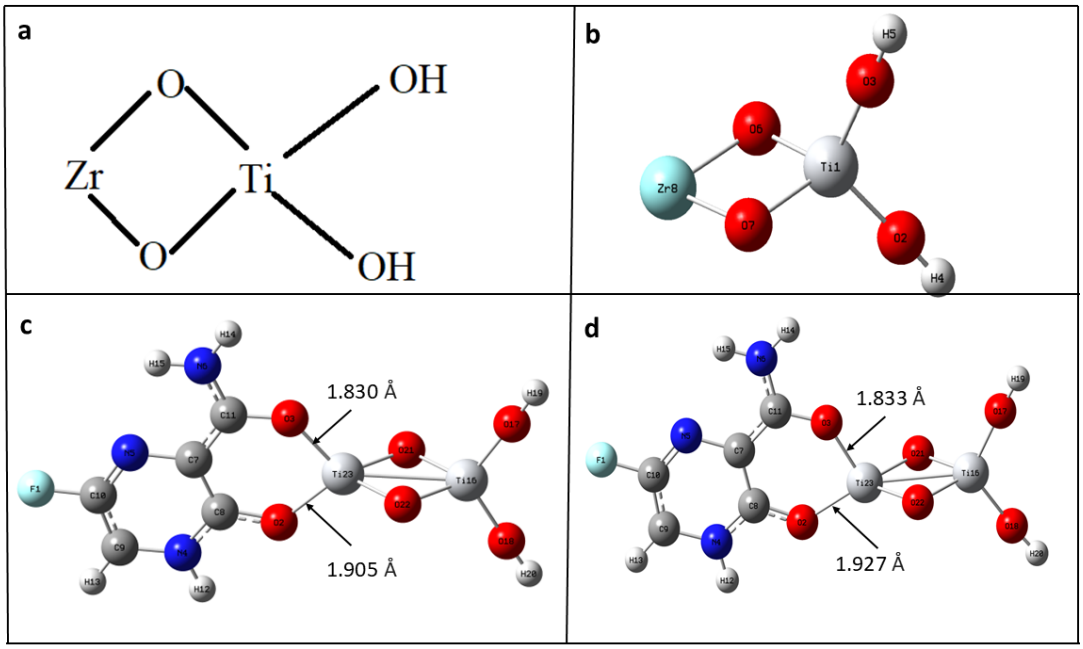

Figure S1 (a) $ZrTiO_4H_2$ nanostructure in two dimensional, (b) $ZrTiO_4H_2$ nanostructure in three dimensional views, (c) optimized structure of Fav+$Ti_2O_4H_2$ in gas phase, and (c) optimized structure of Fav+$ZrTiO_4H_2$ water solvent.

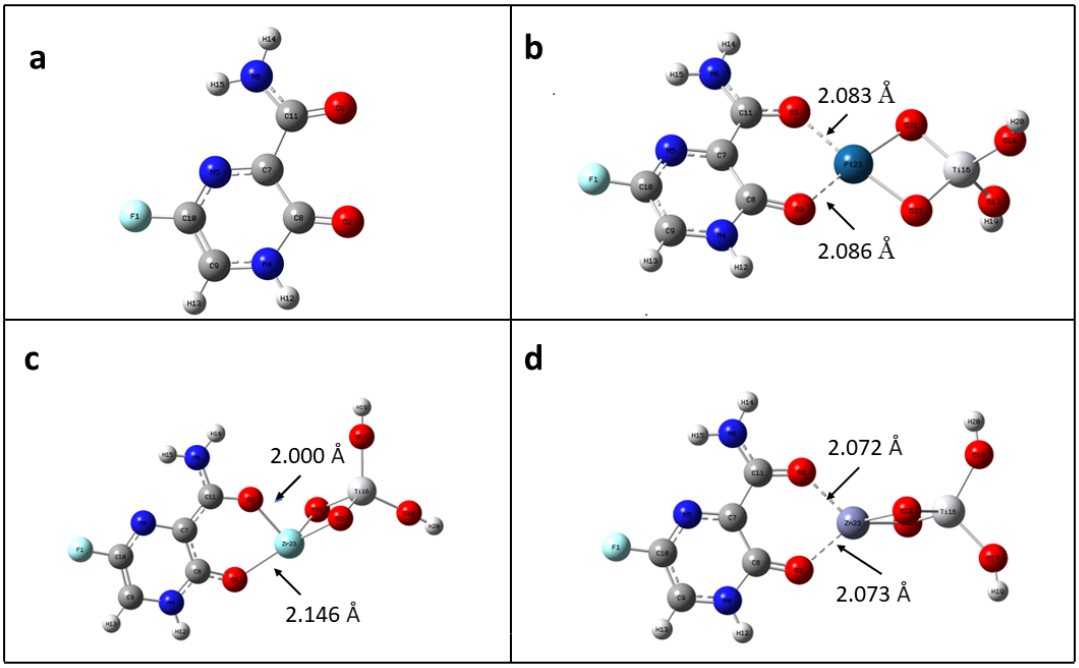

Figure S2 Optimized structure of (a) favipiravir, (b) Fav+$PtTiO_4H_2$, (c) Fav+$ZrTiO_4H_2$, and (d) Fav+$ZnTiO_4H_2$ nanocomplexes in the water solvent.

Table S4 Electronic energy and adsorption energy for Fav+$XTiO_4H_2$ nanocomplex in gas phase and water solvent in B3LYP/LANL2DZ basis set.

Nanocomplex	Medium	Calculated electronic energy (eV)	Adsorption energy (eV)
Fav+$Ti_2O_4H_2$	Gas	-27922.14	-4.65
	Water	-27923.27	-3.23
Fav+$PtTiO_4H_2$ (NC1)	Gas	-29579.21	-2.49
	Water	-29581.13	-1.70
Fav+$ZrTiO_4H_2$ (NC2)	Gas	-27609.26	-4.70
	Water	-27611.62	-3.78
Fav+$ZnTiO_4H_2$ (NC3)	Gas	-28122.70	-2.50
	Water	-28125.41	-1.18

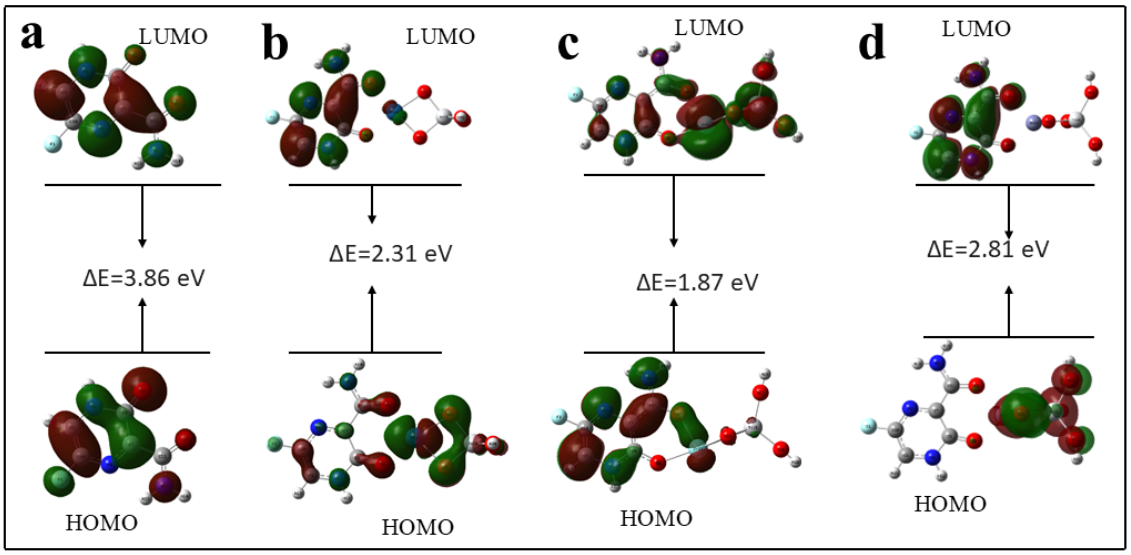

Figure S3 Energy gap of frontier molecular orbitals of (a) favipiravir, (b) Fav+$PtTiO_4H_2$, (c) Fav+$ZrTiO_4H_2$, and (d) Fav+$ZnTiO_4H_2$ nanocomplexes in water solvent.

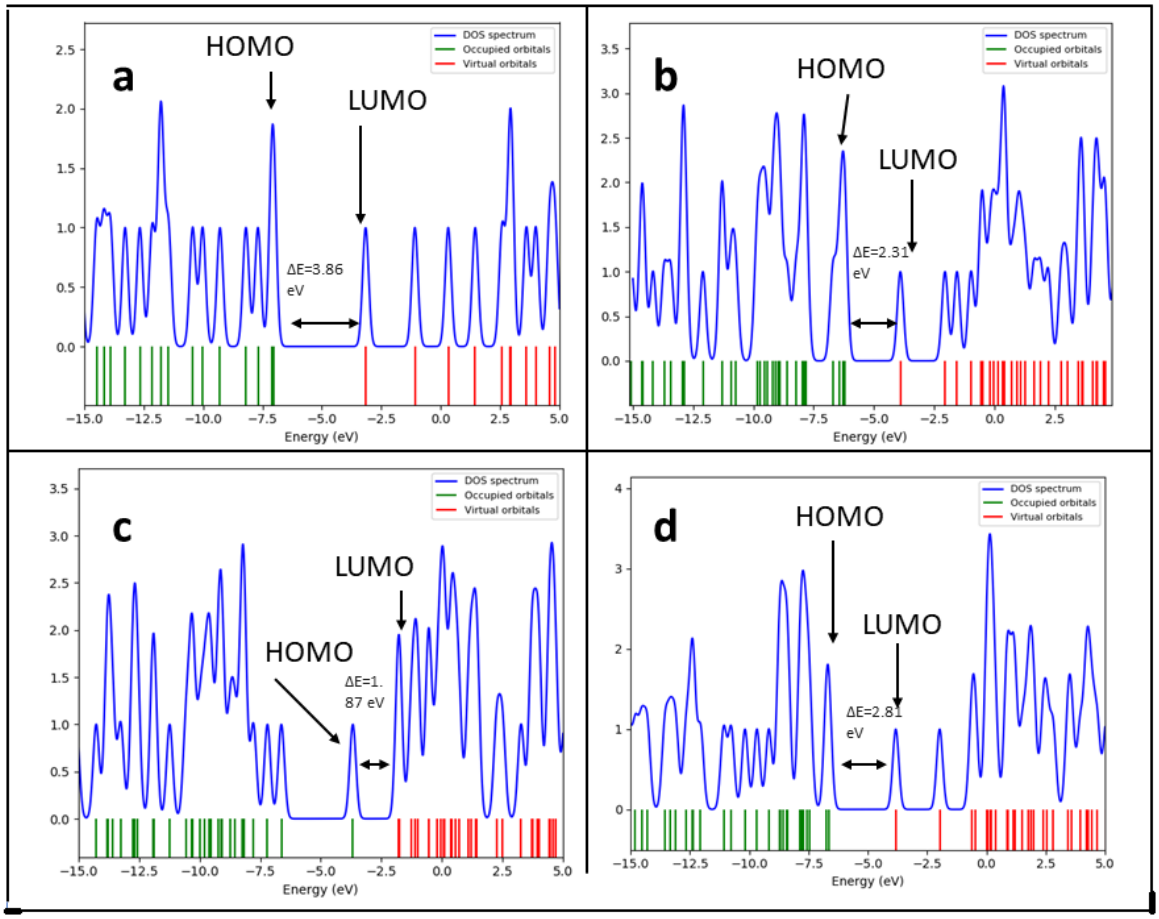

Figure S4 Density of states of (a) favipiravir, (b) Fav+$PtTiO_4H_2$, (c) Fav+$ZrTiO_4H_2$, and (d) Fav+$ZnTiO_4H_2$ nanocomplex in water solvent.

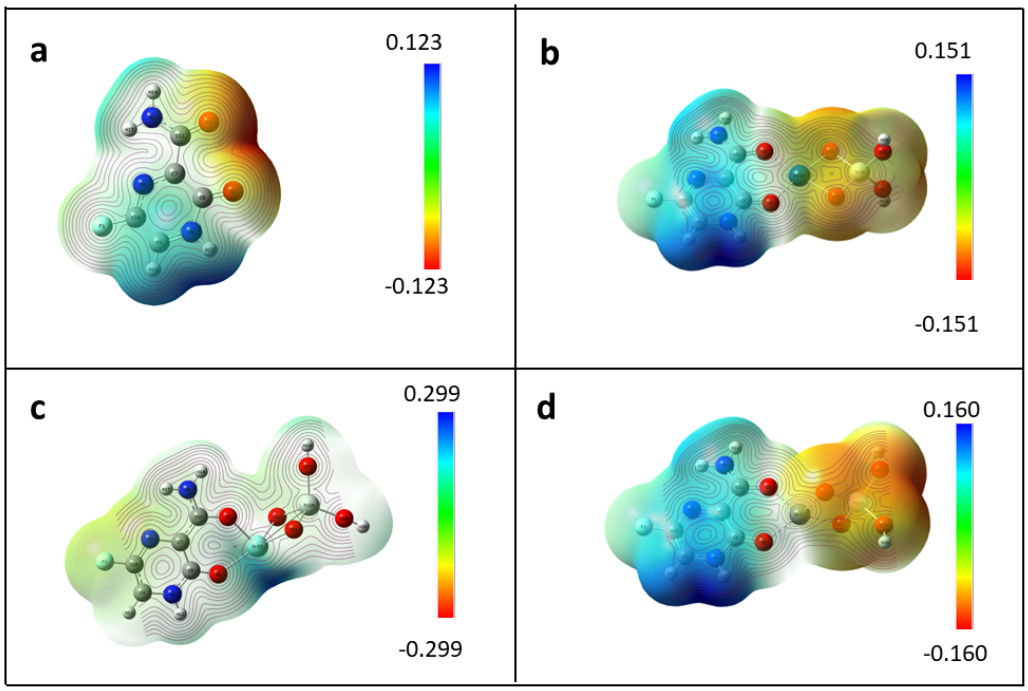

Figure S5 Molecular electrostatic potential diagrams (a) favipiravir, (b) Fav+$PtTiO_4H_2$, (c) Fav+$ZrTiO_4H_2$, and (d) Fav+$ZnTiO_4H_2$ nanocomplex in water solvent.

Table S5 Mulliken and natural charges of favipiravir, Fav+$XTiO_4H_2$ nanocomplexes in gas phase.

Atom	Favipiravir		Fav+$PtTiO_4H_2$ (NC1)		Fav+$ZrTiO_4H_2$ (NC2)		Fav+$ZnTiO_4H_2$ (NC3)	
	Mulliken	**Natural**	**Mulliken**	**Natural**	**Mulliken**	**Natural**	**Mulliken**	**Natural**
F1	-0.20142	-0.36283	-0.19578	-0.35074	-0.22356	-0.37750	-0.18038	-0.34658
O2	-0.21814	-0.58135	-0.30153	-0.60936	-0.59375	-0.83492	-0.39115	-0.68922
O3	-0.24113	-0.59591	-0.32312	-0.60720	-0.58752	-0.82855	-0.40398	-0.70653
N4	-0.35220	-0.60297	-0.35976	-0.57133	-0.29829	-0.54319	-0.33084	-0.56832
N5	0.01442	-0.49785	0.00063	-0.48992	-0.09844	-0.61803	0.01722	-0.48211
N6	-0.63059	-0.85262	-0.63493	-0.81102	-0.66195	-0.86306	-0.60042	-0.79382
C7	-0.01060	0.11121	-0.06830	0.08467	-0.02252	-0.06948	-0.04016	0.07541
C8	0.17706	0.61851	0.35134	0.63452	0.35253	0.61625	0.32741	0.64281
C9	-0.19099	-0.00083	-0.23635	-0.00263	-0.38771	-0.23661	-0.19868	0.00478
C10	0.11955	0.55481	0.13209	0.57515	0.13143	0.63642	0.13434	0.58055
C11	0.19979	0.65590	0.33702	0.67204	0.33308	0.54093	0.34511	0.69484
H12	0.36015	0.45201	0.36691	0.46736	0.34575	0.44795	0.38779	0.46888
H13	0.27763	0.24415	0.28240	0.25346	0.26541	0.23096	0.29491	0.25621
H14	0.33784	0.42467	0.34508	0.44017	0.32056	0.41974	0.36805	0.44252
H15	0.35864	0.43310	0.37466	0.44318	0.36343	0.44387	0.37767	0.44565
Ti16			1.27820	1.34354	1.20435	1.43454	1.11605	1.29730
O17			-0.77189	-0.92861	-0.75503	-0.89458	-0.79965	-0.94143
O18			-0.77323	-0.92861	-0.75662	-0.89665	-0.79534	-0.93973
H19			0.38839	0.51534	0.40448	0.53129	0.36875	0.50716
H20			0.38775	0.51534	0.40368	0.53063	0.36934	0.50694
O21			-0.60671	-0.72385	-0.71905	-0.88452	-0.75310	-0.93882
O22			-0.60133	-0.72698	-0.71906	-0.88453	-0.75304	-0.93881
Pt23/Zr23/Zn23			0.62845	0.80547	1.69878	2.09905	1.14011	1.42232

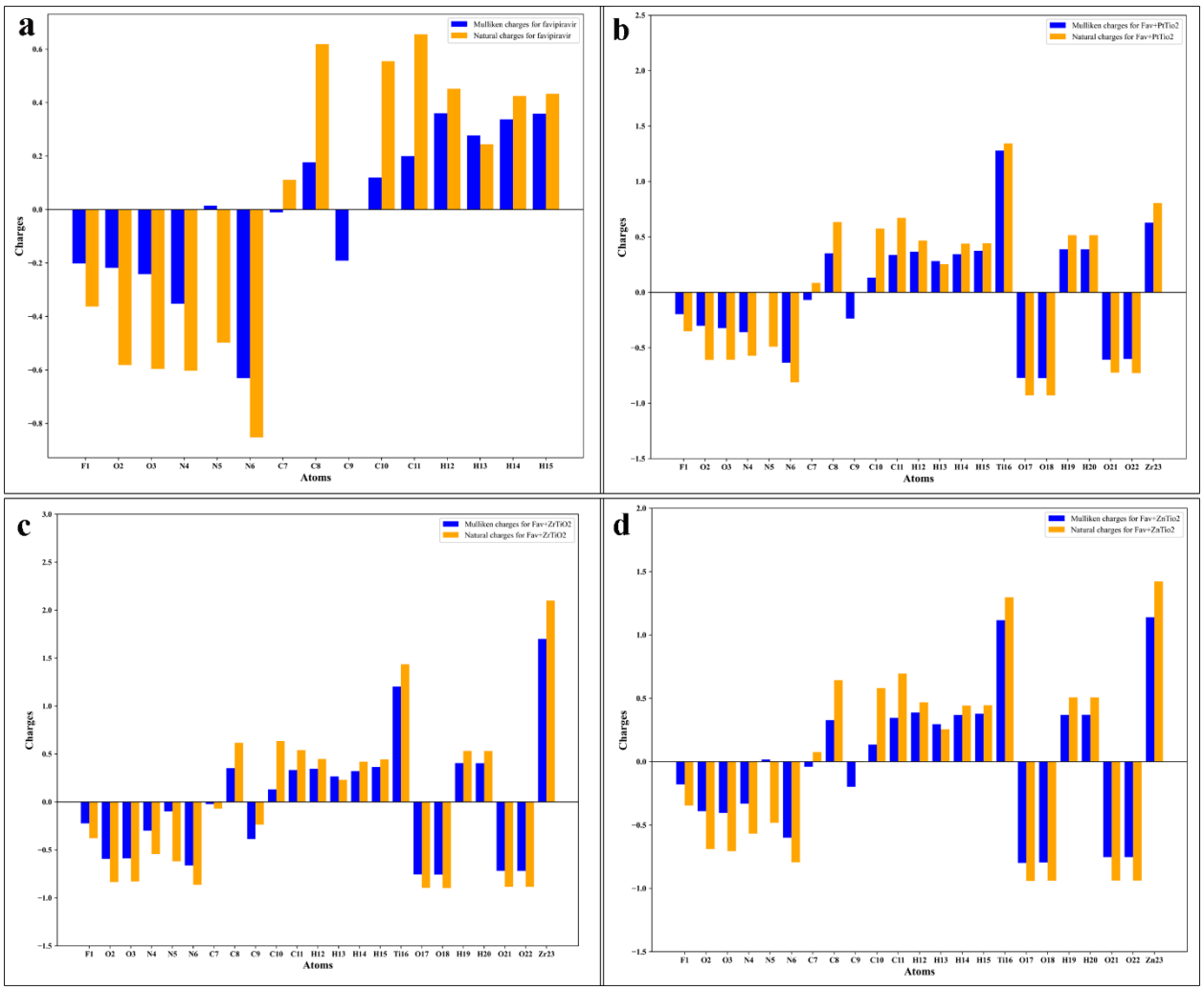

Figure S6 Mulliken and natural charge distribution in (a) favipiravir, (b) Fav+$PtTiO_4H_2$, (c)Fav+$ZrTiO_4H_2$, and (d) Fav+$ZnTiO_4H_2$ nanocomplexes in gas phase.

Table S6 Mulliken and natural charges of favipiravir, Fav+ $XTiO_4H_2$ nanocomplexes in water solvent.

Atom	Favipiravir		Fav+$PtTiO_4H_2$ (NC1)		Fav+$ZrTiO_4H_2$ (NC2)		Fav+$ZnTiO_4H_2$ (NC3)	
	Mulliken	**Natural**	**Mulliken**	**Natural**	**Mulliken**	**Natural**	**Mulliken**	**Natural**
F1	-0.21828	-0.37374	-0.20841	-0.35472	-0.25668	-0.41854	-0.19585	-0.35579
O2	-0.31789	-0.66736	-0.35388	-0.64308	-0.58454	-0.84267	-0.44697	-0.74094
O3	-0.34064	-0.68381	-0.38483	-0.64806	-0.59910	-0.84857	-0.42853	-0.74850
N4	-0.32397	-0.56804	-0.33696	-0.52188	-0.30676	-0.58120	-0.29800	-0.52776
N5	0.00587	-0.49100	0.01208	-0.45413	-0.16735	-0.73361	0.03025	-0.45595
N6	-0.61967	-0.83191	-0.60971	-0.76959	-0.67503	-0.87707	-0.58546	-0.77009
C7	0.01071	0.09225	-0.02542	0.08856	-0.04555	-0.06980	-0.02380	0.09251
C8	0.18456	0.62744	0.40429	0.64714	0.35633	0.65516	0.37095	0.65601
C9	-0.15188	0.04428	-0.16714	0.07823	-0.45131	-0.29740	-0.14732	0.07339
C10	0.12386	0.56163	0.14225	0.58991	0.09646	0.60288	0.14461	0.58890

Atom	Favipiravir		Fav+$PtTiO_4H_2$ (NC1)		Fav+$ZrTiO_4H_2$ (NC2)		Fav+$ZnTiO_4H_2$ (NC3)	
	Mulliken	**Natural**	**Mulliken**	**Natural**	**Mulliken**	**Natural**	**Mulliken**	**Natural**
C11	0.19823	0.66737	0.37565	0.69937	0.30940	0.54930	0.35024	0.70807
H12	0.39992	0.47549	0.41124	0.49441	0.37179	0.45426	0.42447	0.49225
H13	0.31399	0.26857	0.32335	0.28202	0.27830	0.23306	0.32966	0.28064
H14	0.36003	0.43631	0.37786	0.45378	0.34010	0.42832	0.38540	0.45275
H15	0.37517	0.44251	0.39633	0.45734	0.35447	0.43670	0.39505	0.45572
Ti16			1.19096	1.29999	1.18026	1.41473	0.92398	1.21610
O17			-0.80888	-0.96009	-0.77330	-0.92234	-0.83036	-0.98807
O18			-0.80862	-0.96153	-0.77387	-0.92150	-0.83137	-0.98822
H19			0.40611	0.52350	0.42167	0.53909	0.38571	0.51225
H20			0.40624	0.52257	0.42153	0.53921	0.38667	0.51175
O21			-0.67131	-0.79614	-0.76074	-0.92642	-0.80645	-0.99638
O22			-0.66683	-0.79558	-0.76074	-0.92623	-0.80005	-0.98999
Pt23/Zr23/Zn23			0.59565	0.76797	2.02464	2.51264	1.26717	1.52138

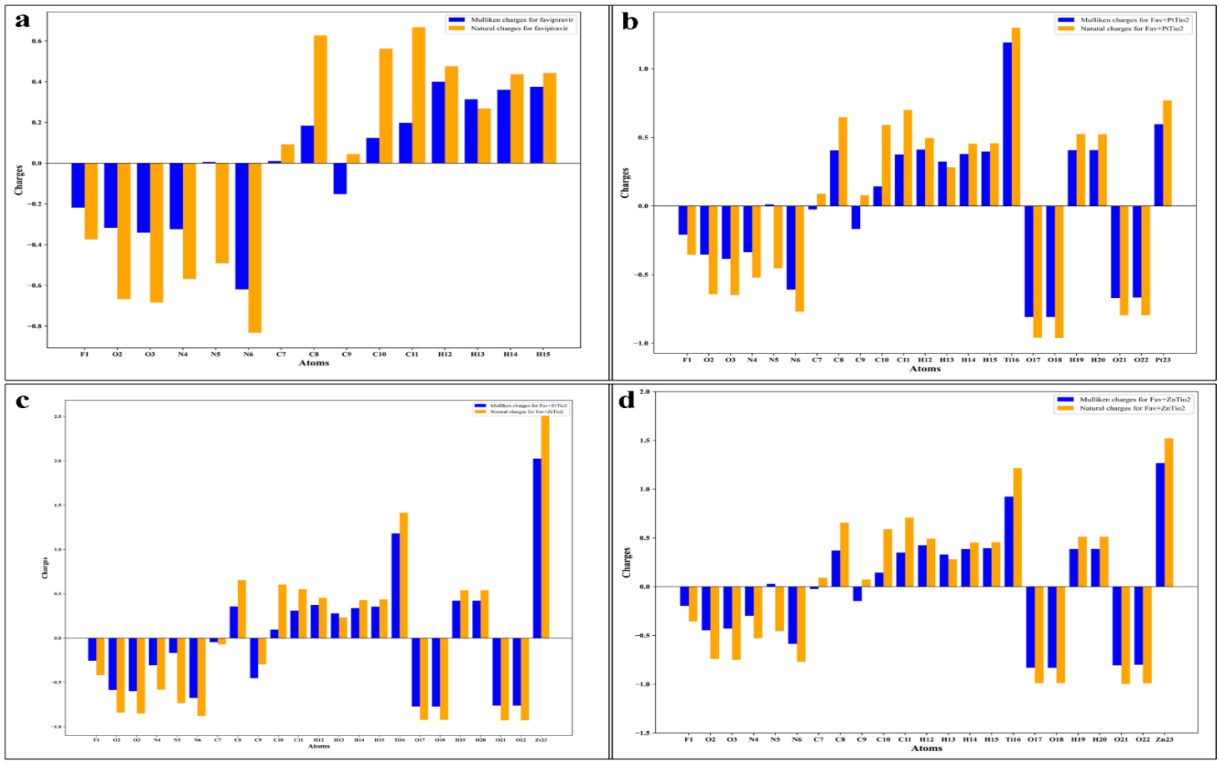

Figure S7 Mulliken and natural charge distribution of (a) favipiravir, (b) Fav+$PtTiO_4H_2$, (c) Fav+Zr TiO_4H_2, and (d) Fav+$ZnTiO_4H_2$ nanocomplexes in water solvent.

Table S7 Thermodynamical properties of favipiravir and Fav+$XTiO_4H_2$ at gas and water solvent using B3LYP/LANL2DZ basis set.

Parameter	Favipiravir		Fav+$PtTiO_4H_2$ (NC1)		Fav+$ZrTiO_4H_2$ (NC2)		Fav+$ZnTiO_4H_2$ (NC3)	
	Gas	Water	Gas	Water	Gas	Water	Gas	Water
Enthalpy ΔH (Hartree)	-607	-607	-1087	-1087	-1014	-1014	-1033	-1033
Gibbs free energy ΔG (Hartree)	-607	-607	-1087	-1087	-1015	-1015	-1033	-1033
Thermal energy ΔE (kcal/mol)	69	69	97	97	95	94	96	96
Specific heat capacity Cv (cal/mol-Kelvin)	34	34	68	68	69	71	69	68
Entropy S (cal/mol-Kelvin)	95	94	144	143	143	146	150	145

Table S8 Favipiravir in gas phase of thermal energy, specific heat capacity, and entropy at temperature ranging from 50 to 500 K.

Temperature (K)	Thermal Energy (kcal/mol)	Heat Capacity (cal/mol-K)	Entropy (cal/mol-K)
50	63.187	9.648	59.992
100	63.765	13.622	69.226
150	64.567	18.614	76.471
200	65.633	24.022	83.137
250	66.967	29.276	89.510
300	68.554	34.162	95.648
350	70.367	38.621	101.561
400	72.409	42.641	107.251
450	74.632	46.231	112.719
500	77.025	49.417	117.967

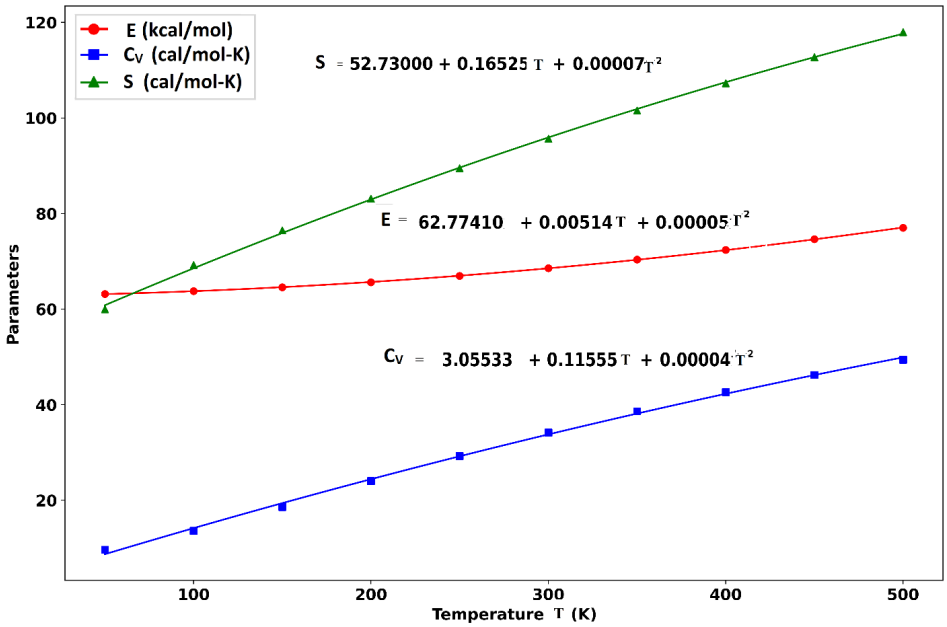

Figure S8 Variation of thermal energy correction (E), specific heat capacity at constant volume (C_v), and entropy (S) with temperature of favipiravir in gas phase.

Table S9 Fav+$PtTiO_4H_2$ in gas phase of thermal energy, specific heat capacity, and entropy at temperature ranging from 50 to 500 K.

Temperature (K)	Thermal Energy (kcal/mol)	Heat Capacity (cal/mol-K)	Entropy (cal/mol-K)
50	85.222	16.914	72.049
100	86.426	30.941	89.553
150	88.271	42.494	105.163
200	90.647	52.310	119.338
250	93.480	60.799	132.389
300	96.708	68.123	144.500
350	100.276	74.438	155.794
400	104.137	79.884	166.363
450	108.252	84.582	176.285
500	112.585	88.640	185.621

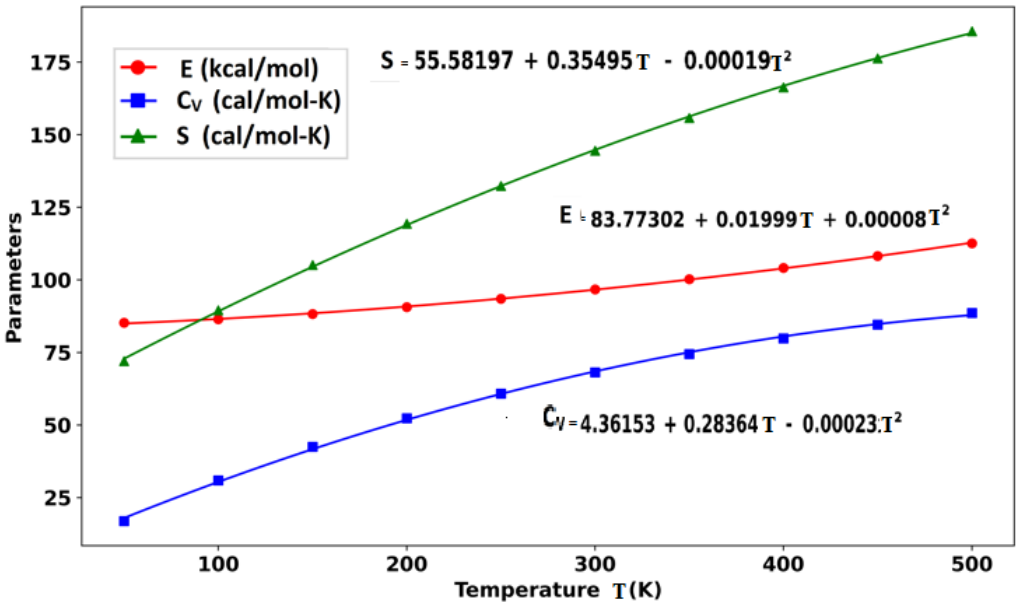

Figure S9 Variation of thermal energy correction (E), specific heat capacity at constant volume (C_v), and entropy (S) with temperature of Fav+$PtTiO_4H_2$ in gas phase.

Table S10 Fav+$ZrTiO_4H_2$ in gas phase of thermal energy, specific heat capacity, and entropy at temperature ranging from 50 to 500 K.

Temperature (K)	Thermal Energy(kcal/mol)	Heat Capacity (cal/mol-K)	Entropy (cal/mol-K)
50	84.221	16.778	72.189
100	85.374	29.427	89.042
150	87.157	41.683	104.137
200	89.516	52.401	118.209
250	92.369	61.453	131.347
300	95.637	69.071	143.607
350	99.256	75.517	155.058
400	103.173	81.001	165.776
450	107.343	85.684	175.828
500	111.730	89.696	185.278

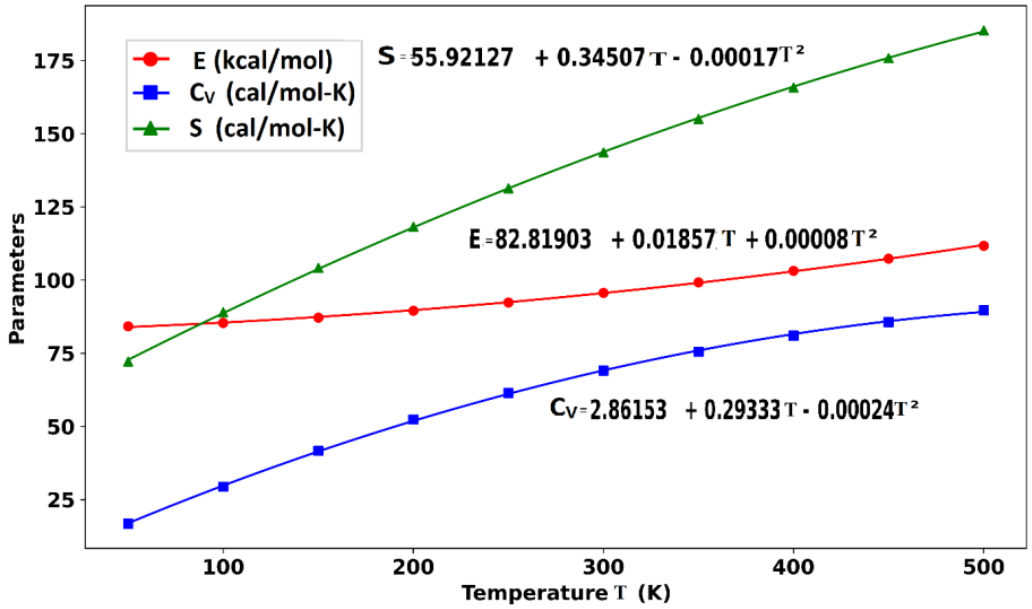

Figure S10 Variation of thermal energy correction (E), specific heat capacity at constant volume (C_v), and entropy (S) with temperature of Fav+$ZrTiO_4H_2$ in gas phase.

Table S11 Fav+$ZnTiO_4H_2$ in gas phase of thermal energy, specific heat capacity at constant volume, and entropy at temperature ranging from 50 to 500 K.

Temperature (K)	Thermal Energy (kcal/mol)	Heat Capacity (cal/mol-K)	Entropy (cal/mol-K)
50	84.683	19.166	74.744
100	86.015	33.427	94.019
150	87.969	44.333	110.515
200	90.423	53.619	125.142
250	93.311	61.736	138.443
300	96.579	68.802	150.700
350	100.176	74.935	162.084
400	104.059	80.251	172.711
450	108.189	84.854	182.670
500	112.534	88.842	192.031

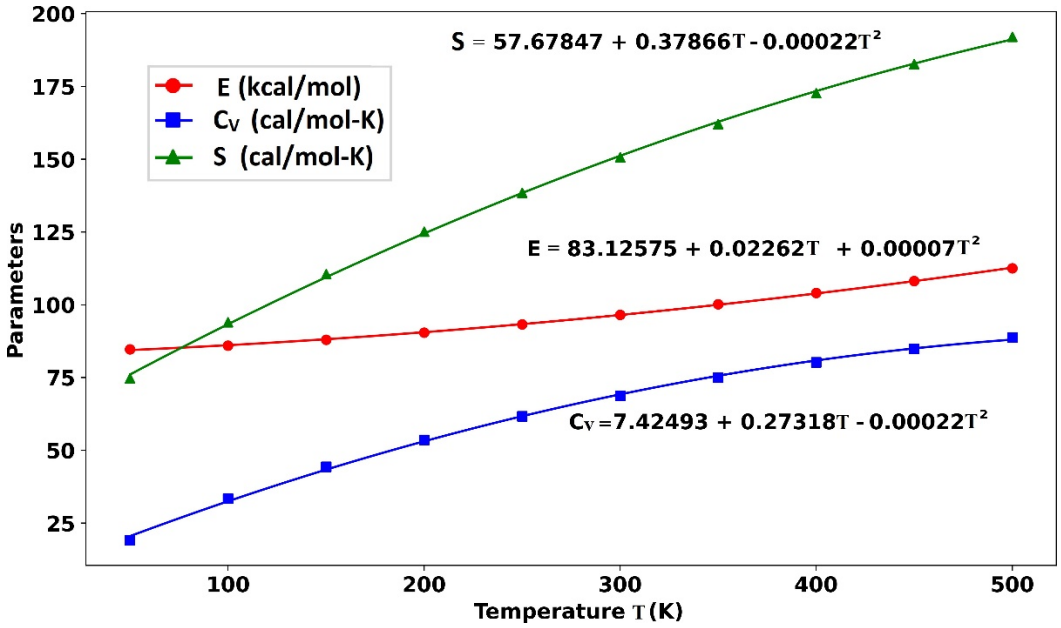

Figure S11 Variation of thermal energy correction (E), molar heat capacity at constant volume (Cv), and entropy (S) with temperature of Fav+$ZnTiO_4H_2$ in gas phase.

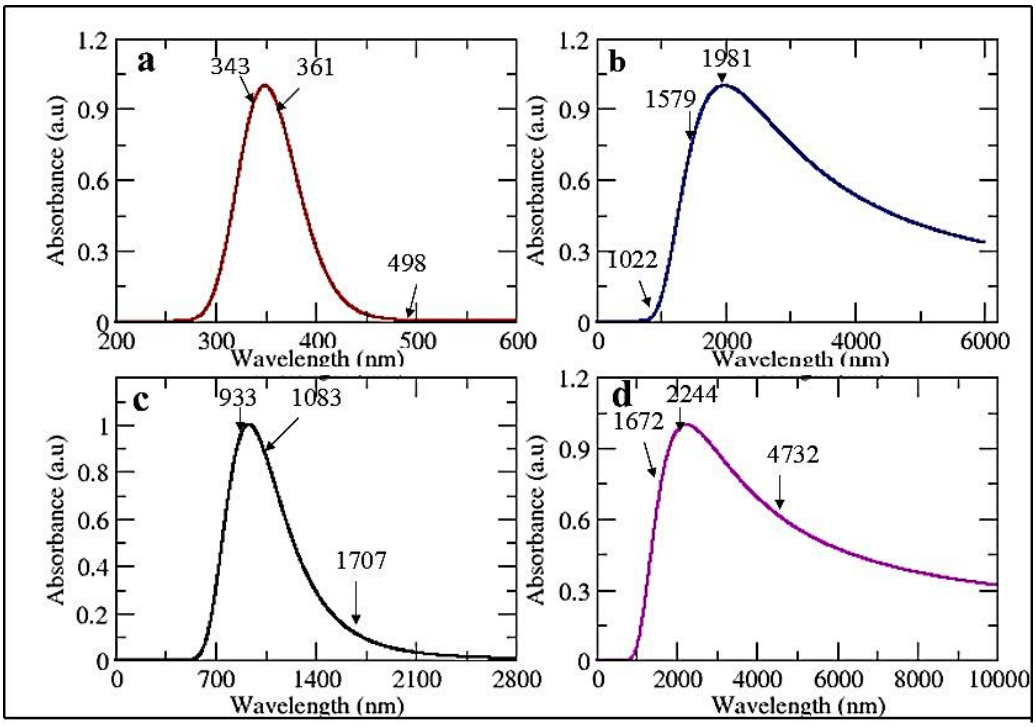

Figure S12 Calculated ultraviolet-visible spectra of (a) favipiravir, (b) Fav+$PtTiO_4H_2$, (c) Fav+$ZrTiO_4H_2$, and (d) Fav+$ZnTiO_4H_2$ nanocomplexes in gas phase.

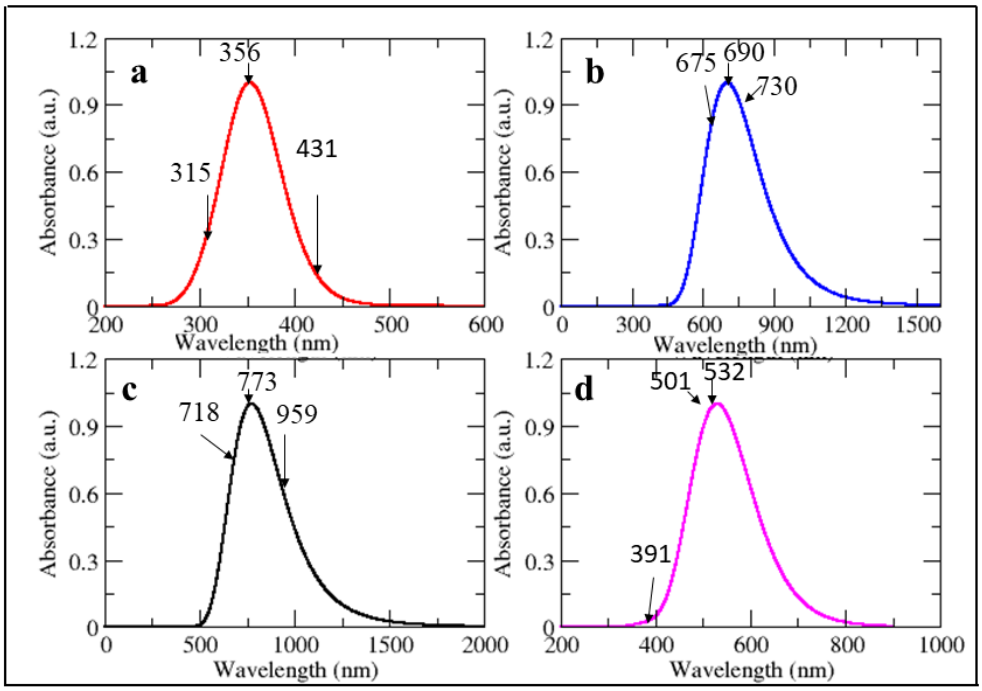

Figure S13 Calculated ultraviolet-visible spectra of (a) favipiravir, (b) Fav+$PtTiO_4H_2$, (c) Fav+Zr TiO_4H_2, and (d) Fav+$ZnTiO_4H_2$ nanocomplexes in water solvent.

Table S12 Calculated electronic properties of favipiravir and $XTiO_4H_2$ nanocomplex in gas and water solvent.

Parameter	Gas Phase		Water solvent	
	Maximum absorption wavelength (nm)	Oscillator strength	Maximum absorption wavelength (nm)	Oscillator strength
Favipiravir	498	0.00	431	0.00
	361	0.06	356	0.17
	343	0.06	315	0.03
Fav+$PtTiO_4H_2$	1981	0.01	730	0.02
(NC1)	1579	0.00	690	0.03
	1021	0.00	675	0.00
Fav+$ZrTiO_4H_2$	1707	0.00	959	0.00
(NC2)	1082	0.00	773	0.17
	933	0.13	718	0.00
Fav+$ZnTiO_4H_2$	4734	0.00	532	0.01
(NC3)	2244	0.05	501	0.00
	1672	0.00	391	0.00

Table S13 Local reactive descriptors of atoms in favipiravir to explain their reactive sites calculated at B3LYP/LANL2DZ level of theory.

Atom	Nucleophilic attack (f_k^+)	Electrophilic attack (f_k^-))	Radial attack (f_k^0))	Dual descriptor (Δf_k)
F1	-0.04590	-0.20225	-0.12408	0.15635
O2	-0.10313	-0.22203	-0.16258	0.11890
O3	-0.10485	-0.18286	-0.14386	0.07801
N4	-0.06569	-0.30741	-0.18655	0.24172
N5	-0.14500	-0.26386	-0.20443	0.11886
N6	-0.04610	-0.45842	-0.25226	0.41232
C7	-0.17812	0.09498	-0.04157	-0.27310
C8	0.01224	0.28767	0.14996	-0.27543
C9	-0.18763	-0.03205	-0.10984	-0.15558
C10	0.00480	0.27124	0.13802	-0.26644
C11	-0.00526	0.30468	0.14971	-0.30994
H12	-0.04438	0.20968	0.08265	-0.25406
H13	-0.04669	0.10336	0.02834	-0.15005
H14	-0.03540	0.19553	0.08007	-0.23093
H15	-0.00889	0.20171	0.09641	-0.21060

Table S14 Local reactive descriptors of atoms in Fav+$PtTiO_4H_2$ to explain their reactive sites calculated at B3LYP/LANL2DZ level of theory.

Atom	Nucleophilic attack (f_k^+)	Electrophilic attack (f_k^-))	Radial attack (f_k^0))	Dual descriptor (Δf_k)
F1	-0.03901	-0.03076	-0.03489	-0.00825
O2	-0.04807	0.01798	-0.01505	-0.06605
O3	-0.06175	0.02509	-0.01833	-0.08684
N4	-0.05372	-0.03503	-0.04438	-0.01869
N5	-0.11773	-0.05826	-0.08800	-0.05947
N6	-0.04056	-0.05241	-0.04649	0.01185
C7	-0.13862	-0.00036	-0.06949	-0.13826
C8	0.01136	-0.01354	-0.00109	0.0249
C9	-0.15143	-0.05919	-0.10531	-0.09224
C10	0.00388	-0.02359	-0.00986	0.02747
C11	0.00193	-0.02349	-0.01078	0.02542
H12	-0.03405	-0.01881	-0.02643	-0.01524
H13	-0.03853	-0.02475	-0.03164	-0.01378
H14	-0.02581	-0.01613	-0.02097	-0.00968
H15	-0.00862	-0.01341	-0.01102	0.00479
Ti16	-0.04640	-0.05638	-0.05139	0.00998
O17	-0.02404	-0.05951	-0.04178	0.03547
O18	-0.02404	-0.05952	-0.04178	0.03548
H19	-0.01598	-0.02581	-0.02090	0.00983
H20	-0.01598	-0.02581	-0.02090	0.00983
O21	-0.03659	-0.04869	-0.04264	0.0121
O22	-0.02539	-0.16850	-0.09695	0.14311
Pt23	-0.07084	-0.22915	-0.15000	0.15831

Table S15 Local reactive descriptors of atoms in Fav+$ZrTiO_4H_2$ to explain their reactive sites calculated at B3LYP/LANL2DZ level of theory.

Atom	Nucleophilic attack (f_k^+)	Electrophilic attack (f_k^-))	Radial attack (f_k^0))	Dual descriptor (Δf_k)
F1	-0.02679	-0.03722	-0.03201	0.01043
O2	-0.00156	-0.01923	-0.01040	0.01767
O3	-0.02482	-0.00946	-0.01714	-0.01536
N4	-0.03004	0.00695	-0.01155	-0.03699
N5	-0.07536	-0.10967	-0.09252	0.03431
N6	-0.01301	-0.10612	-0.05957	0.09311
C7	-0.01935	-0.03070	-0.02503	0.01135
C8	0.02319	-0.02588	-0.00134	0.04907
C9	-0.10058	-0.18596	-0.14327	0.08538
C10	-0.00698	0.00921	0.00111	-0.01619
C11	0.01657	-0.09362	-0.03853	0.11019
H12	-0.01934	-0.02415	-0.02175	0.00481
H13	-0.02264	-0.03006	-0.02635	0.00742
H14	-0.01206	-0.02967	-0.02087	0.01761
H15	-0.01015	-0.01719	-0.01367	0.00704
Ti16	-0.19858	-0.03977	-0.11918	-0.15881
O17	-0.04984	-0.03097	-0.04041	-0.01887
O18	-0.04894	-0.03150	-0.04022	-0.01744
H19	-0.03168	-0.01524	-0.02346	-0.01644
H20	-0.03179	-0.01561	-0.02370	-0.01618
O21	-0.03789	-0.02233	-0.03011	-0.01556
O22	-0.03789	-0.02234	-0.03012	-0.01555
Zr23	-0.24048	-0.11944	-0.17996	-0.12104

Table S16 Local reactive descriptors of atoms in Fav+$ZnTiO_4H_2$ to explain their reactive sites calculated at B3LYP/LANL2DZ level of theory.

Atom	Nucleophilic attack (f_k^+)	Electrophilic attack (f_k^-))	Radial attack (f_k^0))	Dual descriptor (Δf_k)
F1	-0.04070	-0.02293	-0.03182	-0.01777
O2	-0.06436	0.03276	-0.01580	-0.09712
O3	-0.07075	0.03237	-0.01919	-0.10312
N4	-0.05705	-0.02243	-0.03974	-0.03462
N5	-0.12371	-0.04536	-0.08454	-0.07835
N6	-0.05101	-0.03234	-0.04168	-0.01867
C7	-0.13045	-0.00691	-0.06868	-0.12354
C8	0.00875	-0.00734	0.00071	0.01609
C9	-0.15626	-0.04770	-0.10198	-0.10856

Atom	Nucleophilic attack (f_k^+)	Electrophilic attack (f_k^-))	Radial attack (f_k^0))	Dual descriptor (Δf_k)
C10	0.00185	-0.01267	-0.00541	0.01452
C11	-0.00985	-0.01338	-0.01162	0.00353
H12	-0.03599	-0.01180	-0.02390	-0.02419
H13	-0.04021	-0.01862	-0.02942	-0.02159
H14	-0.02853	-0.01060	-0.01957	-0.01793
H15	-0.00977	-0.01074	-0.01026	0.00097
Ti16	-0.04074	-0.05436	-0.04755	0.01362
O17	-0.02110	-0.07415	-0.04763	0.05305
O18	-0.02203	-0.07646	-0.04925	0.05443
H19	-0.01461	-0.03249	-0.02355	0.01788
H20	-0.01477	-0.03227	-0.02352	0.0175
O21	-0.04156	-0.23777	-0.13967	0.19621
O22	-0.04156	-0.23778	-0.13967	0.19622
Zn23	0.00441	-0.05703	-0.02631	0.06144

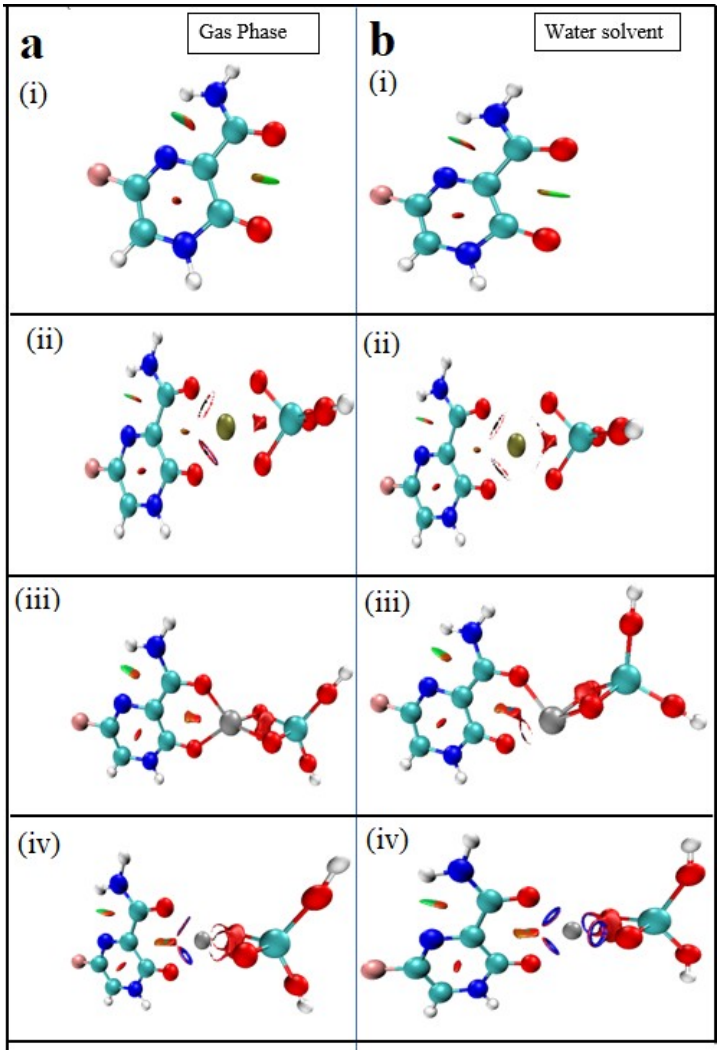

Figure S14 Non-covalent interaction in isosurface of (i) favipiravir, (ii) Fav+$PtTiO_4H_2$, (iii) Fav+$ZrTiO_4H_2$, and (iv) Fav+$ZnTiO_4H_2$ nanocomplexes in a. gas phase and b.water solvent.

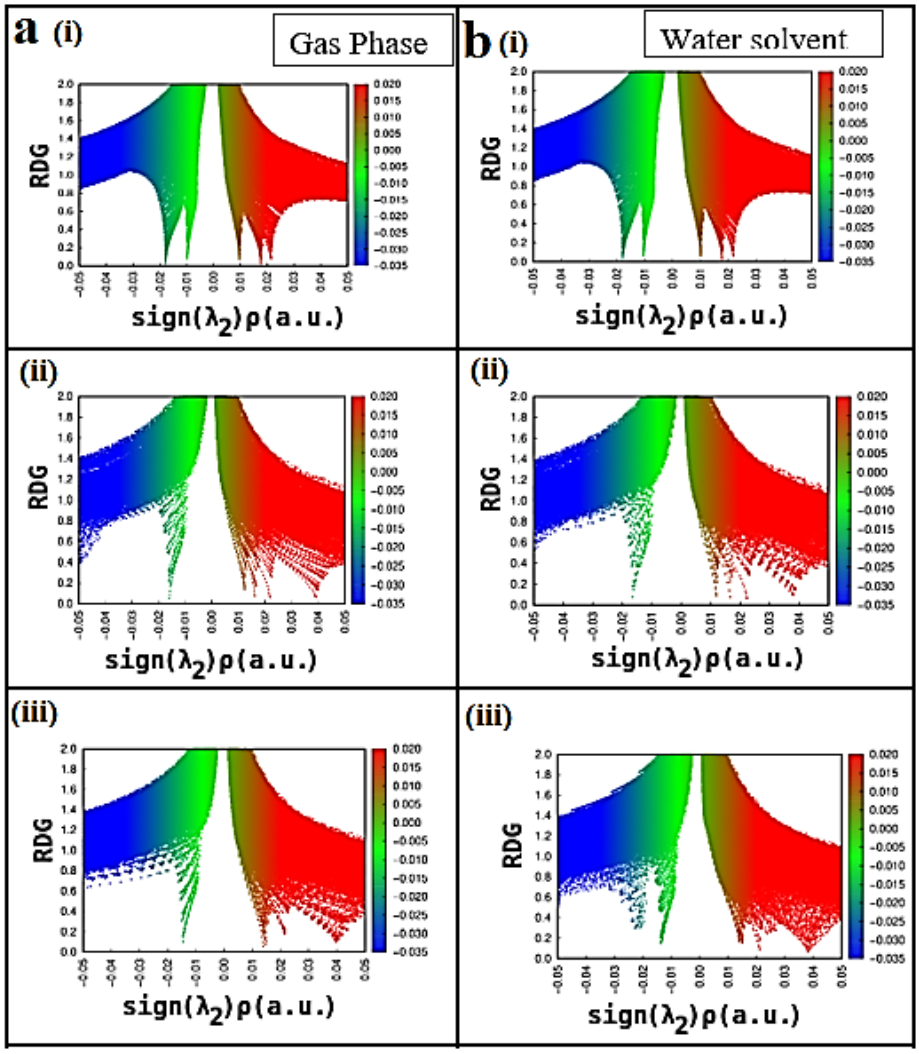

Figure S15 RDG scatter graph of (i) favipiravir (ii) Fav+ $PtTiO_4H_2$ (iii) Fav+$ZrTiO_4H_2$ nanocomplexes in a. gas phase and b. water solvent.

Table S17 Second order perturbation theory analysis of Fock matrix on NBO basis for favipiravir.

Donor NBO (i)	Type	Acceptor NBO (j)	Type	E(2)kcal/mol	E(j)-E(i) a.u.	F(i,j) a.u.
N6	LP(1)	O3 - C11	π*	67.25	0.25	0.12
N4	LP(1)	O2 - C8	π*	43.73	0.28	0.10
N4	LP(1)	C9 - C10	π*	43.43	0.28	0.10
O2	LP(2)	N4 - C8	σ*	28.42	0.56	0.11
O3	LP(2)	N6 - C11	σ*	21.05	0.66	0.11
C9 - C10	π	N5 - C7	π*	20.64	0.30	0.07
O3	LP(2)	C7 - C11	σ*	20.31	0.61	0.10
N5 - C7	π	C9 - C10	π*	19.34	0.32	0.07
O2	LP(2)	C7 - C8	σ*	18.51	0.64	0.10
F1	LP(3)	C9 - C10	π*	16.57	0.39	0.08
N5 - C7	π	O2 - C8	π*	15.50	0.33	0.07
N5	LP(1)	C7 - C8	σ*	12.79	0.75	0.09

Donor NBO (i)	Type	Acceptor NBO (j)	Type	E(2)kcal/mol	E(j)-E(i) a.u.	F(i,j) a.u.
N5 - C7	π	O3 - C11	π*	12.30	0.35	0.06
N5	LP(1)	C 9 - C10	σ*	9.85	0.87	0.08
N5	LP(1)	F1 - C10	σ*	9.34	0.53	0.06
O3 - C11	π	N5 - C7	π*	7.69	0.31	0.05
F1	LP(2)	N5 - C10	σ*	7.40	0.86	0.07
O2 - C8	π	N5 - C7	π*	7.22	0.33	0.05
C9 - H13	σ	N4 - C8	σ*	6.21	0.90	0.07
C7 - C11	σ	N5 - C10	σ*	6.14	1.10	0.07
C9 - H13	σ	N5 - C10	σ*	5.09	1.03	0.07
F1	LP(2)	C9 - C10	σ*	4.94	0.92	0.06
N6 - H14	σ	C 7 - C11	σ*	4.42	1.03	0.06
N6 - H15	σ	O3 - C11	σ*	4.31	1.18	0.06
N4 - C9	σ	F1 - C10	σ*	3.78	1.04	0.06
O2	LP(1)	C7 - C8	σ*	3.77	1.07	0.06
C9 - C10	σ	N4 - H12	σ*	3.74	1.20	0.06
C7 - C11	σ	N6 - H14	σ*	3.63	1.14	0.06
N4 - H12	σ	C9 - C10	σ*	3.33	1.21	0.06
N5 - C10	σ	C7 - C11	σ*	3.32	1.26	0.06
N5 - C7	σ	F1 - C10	σ*	3.26	1.06	0.05
F1 - C10	σ	N 5 - C7	σ*	3.20	1.43	0.06
N5	LP(1)	C7 - C11	σ*	3.08	0.74	0.04
C7 - C8	σ	N4 - H12	σ*	3.05	1.12	0.05
N4 - H12	σ	C7 - C8	σ*	3.00	1.09	0.05
N4 - C8	σ	C7 - C11	σ*	2.78	1.19	0.05
O2 - C8	σ	N4 - C9	σ*	2.76	1.41	0.06
N6 - C11	σ	C7 - C8	σ*	2.61	1.20	0.05
O3	LP(1)	C7 - C11	σ*	2.60	1.04	0.05

Table S18 Second order perturbation theory analysis of Fock matrix on NBO basis for Fav+$PtTiO_4H_2$.

Donor NBO(i)	Type	Acceptor NBO (j)	Type	E(2) kcal/mol	E(j)-E(i) a.u.	F(i,j) a.u.
N5	LP(2)	C7	LP*(1)	380.16	0.07	0.15
C10	LP(1)	N4-C9	π*	233.60	0.08	0.14
N6	LP(1)	O3-C11	π*	81.31	0.22	0.12
O22-Pt23	σ	O2-Pt23	σ*	35.94	0.53	0.13
O21-Pt23	σ	O3-Pt23	σ*	35.58	0.56	0.13
O21-Pt23	σ	Ti16	LP*(2)	28.70	0.72	0.13
O22-Pt23	σ	Ti16	LP*(2)	27.53	0.71	0.13
N4-C9	π	O2-C8	π*	26.76	0.33	0.09
O22-Pt23	σ	Ti16	LP*(1)	20.73	0.34	0.08
O22	LP(1)	Ti16	LP*(3)	20.34	0.83	0.12

Donor NBO(i)	Type	Acceptor NBO (j)	Type	E(2) kcal/mol	E(j)-E(i) a.u.	F(i,j) a.u.
O21-Pt23	σ	Ti16	LP*(1)	19.50	0.36	0.08
O3-Pt23	σ	O21-Pt23	σ*	16.50	0.85	0.11
O2-Pt23	σ	O22-Pt23	σ*	15.61	0.81	0.10
O22 -Pt23	σ	O21-Pt23	σ*	14.66	0.61	0.09
O21 -Pt23	σ	O22-Pt23	σ*	14.04	0.63	0.09
O21	LP(1)	Ti16	LP*(3)	13.70	0.82	0.10
O3	LP(1)	C7-C11	σ*	13.32	0.88	0.10
O2	LP(1)	C7-C8	σ*	13.21	0.94	0.10
O2 -Pt23	σ	N4-C8	σ*	12.49	0.86	0.09
N5	LP(1)	C7-C8	σ*	12.31	0.77	0.09
O17	LP(2)	Ti16-O21	π*	11.99	0.30	0.05
O18	LP(2)	Ti16-O21	π*	11.99	0.30	0.05
O17	LP(1)	Ti16	LP*(1)	11.07	0.24	0.05
O18	LP(1)	Ti16	LP*(1)	11.07	0.24	0.05
O22 -Pt23	σ	Ti16-O22	σ*	10.15	0.70	0.08
N5	LP(1)	C9-C10	σ*	9.95	0.87	0.09
O17	LP(1)	Ti16-O22	π*	9.58	0.30	0.05
O18	LP(1)	Ti16-O22	π*	9.58	0.30	0.05
O3 -Pt23	σ	N6-C11	σ*	9.35	1.00	0.09
Ti16 - O22	σ	O22-Pt23	σ*	9.15	0.86	0.08
O21 -Pt23	σ	Ti16-O21	σ*	9.04	0.68	0.07
O3 - C11	π	C7	LP*(1)	8.92	0.21	0.05
C10	LP(1)	C7	LP*(1)	8.80	0.02	0.01
N5	LP(1)	F1-C10	σ*	8.77	0.54	0.06

Table S19 Second order perturbation theory analysis of Fock matrix on NBO basis for Fav+$ZrTiO_4H_2$.

Donor NBO (i)	Type	Acceptor NBO (j)	Type	E(2) kcal/mol	E(j)-E(i) a.u.	F(i,j) a.u.
C7	LP(1)	O2 - C8	π*	599.80	0.03	0.13
C7	LP(1)	N6 - C11	π*	304.29	0.08	0.14
O22	LP(1)	Zr23	LP*(2)	42.16	0.90	0.17
Ti16 - O22	π	Zr23	LP*(2)	42.10	0.55	0.14
C7	LP(1)	N 5 - C10	π*	40.70	0.13	0.07
N4 - C9	π	O2 - C8	π*	36.79	0.25	0.10
O2	LP(2)	Zr23	LP*(4)	35.59	0.78	0.15
O3	LP(2)	Zr23	LP*(3)	34.41	1.11	0.18
O3 -Zr23	σ	N6 - C11	π*	31.86	0.29	0.11
Ti16 - O21	σ	Zr23	LP*(5)	26.94	1.43	0.18
Ti16 - O22	σ	Zr23	LP*(5)	24.77	1.42	0.17
O21 -Zr23	σ	Ti16 - O22	π*	23.76	0.44	0.09
O2	LP(1)	Zr23	LP*(4)	21.40	0.67	0.11
Ti16 - O22	π	O3 -Zr23	σ*	19.34	0.46	0.09
F1	LP(3)	N5 - C10	π*	19.13	0.39	0.09

Donor NBO (i)	Type	Acceptor NBO (j)	Type	E(2) kcal/mol	E(j)-E(i) a.u.	F(i,j) a.u.
O2	LP(2)	Zr23	LP*(3)	17.77	1.12	0.13
Ti16 - O22	π	Zr23	LP*(3)	17.20	0.93	0.12
O3	LP(2)	Zr23	LP*(4)	16.34	0.77	0.10
O2	LP(2)	O22 -Zr23	σ*	16.12	0.61	0.09
Ti16 - O22	σ	Zr23	LP*(2)	15.20	0.67	0.09
N4 - C9	π	N5 - C10	π*	14.15	0.36	0.07
O3	LP(1)	Zr23	LP*(4)	11.74	0.66	0.08
O3	LP(1)	Zr23	LP*(3)	11.73	1.00	0.10
N5	LP(1)	C9 - C10	σ*	11.70	0.84	0.09
N5 - C10	π	N4 - C9	π*	10.64	0.23	0.06
O21	LP(1)	O21 -Zr23	σ*	10.48	0.97	0.09
Zr23	LP(1)	Zr23	LP*(3)	10.26	0.53	0.15
O21 -Zr23	σ	Ti16	LP*(1)	9.54	1.20	0.10
O3	LP(1)	Zr23	LP*(2)	9.40	0.62	0.07
O2	LP(2)	O21 -Zr23	π*	9.27	0.61	0.07
N5	LP(1)	C7 - C8	σ*	9.26	0.78	0.08
O2	LP(1)	C7 - C8	σ*	9.07	0.96	0.08
N5	LP(1)	F1 - C10	σ*	9.01	0.52	0.06
Ti16 - O21	σ	O21 -Zr23	σ*	8.71	0.76	0.07

Table S20 Second order perturbation theory analysis of Fock matrix on NBO basis for Fav+$ZnTiO_4H_2$.

Donor NBO (i)	Type	Acceptor NBO(j)	Type	E(2) kcal/mol	E(j)-E(i) a.u.	F(i,j) a.u.
N5	LP(2)	C7	LP*(1)	384.30	0.07	0.15
C10	LP(1)	N4 - C9	π*	224.90	0.08	0.13
N6	LP(1)	O3 - C11	π*	86.98	0.22	0.13
Ti16 - O21	BD(3)	Zn23	LP*(6)	66.40	0.74	0.20
O22	LP(2)	Zn23	LP*(6)	32.83	0.73	0.14
F1	LP(3)	C10	LP(1)	29.95	0.23	0.10
N4 - C9	π	O2 - C 8	π*	26.97	0.33	0.09
O21	LP(1)	Ti16	LP*(2)	26.50	0.95	0.14
Ti16 - O21	BD(3)	Zn23	LP*(8)	24.82	0.72	0.12
Ti16 - O22	σ	Zn23	LP*(8)	22.39	1.02	0.14
Ti16 - O21	σ	Zn23	LP*(8)	21.41	1.02	0.14
O2	LP(2)	N4 - C8	σ*	19.43	0.74	0.11
O22	LP(2)	Ti16 - O21	BD*(3)	18.66	0.35	0.08
O3	LP(2)	Zn23	LP*(6)	17.97	1.01	0.12
O2	LP(2)	Zn23	LP*(6)	15.31	0.94	0.11
O21	LP(1)	Zn23	LP*(7)	14.92	0.83	0.10
O22	LP(2)	Zn23	LP*(8)	14.84	0.71	0.10
O22	LP(1)	Ti16	LP*(1)	14.76	1.14	0.12

Donor NBO (i)	Type	Acceptor NBO(j)	Type	E(2) kcal/mol	E(j)-E(i) a.u.	F(i,j) a.u.
O22	LP(1)	Zn23	LP*(7)	14.70	0.83	0.10
O22	LP(2)	Zn23	LP*(7)	13.39	0.39	0.07
O3	LP(2)	N6 - C11	σ*	13.36	0.91	0.10
Ti16 - O21	BD(3)	Ti16	LP*(1)	12.94	0.72	0.09
N5	LP(1)	C7 - C8	σ*	12.43	0.78	0.09
Ti16 - O21	BD(3)	Zn23	LP*(7)	11.87	0.41	0.06
O3	LP(1)	C 7 - C11	σ*	11.84	0.91	0.09
O3	LP(2)	Zn23	LP*(8)	11.26	0.99	0.09
Ti16 - O22	σ	Zn23	LP*(6)	10.79	1.04	0.10
O2	LP(1)	Zn23	LP*(9)	10.67	0.85	0.09
O17	LP(2)	Ti16 - O21	π*	10.31	0.29	0.05
O2	LP(1)	C7 - C8	σ*	10.28	1.01	0.09
O17	LP(2)	Ti16 - O22	π*	10.19	0.29	0.05
O18	LP(2)	Ti16 - O22	π*	10.02	0.29	0.05
N5	LP(1)	C9 - C10	σ*	9.97	0.86	0.08
O18	LP(2)	Ti16 - O21	π*	9.91	0.29	0.05

Table S21 Interaction of Mpro protein residues with favipiravir, Fav+$XTiO_4H_2$ nanocomplex.

Ligand	Target Protein	Binding residue	Atoms	Bond length(Å)	Interaction
Favipiravir	Mpro	Thr190	NH-O	2.03	H-bond
		Gln192	HN-O	2.05	H-bond
		Glu166, Leu167, Gln189			van der Waal bond
		Pro168, Arg188, Ala191			carbon hydrogen bond
		Met165			pi-Alkyl
Fav+$PtTiO_4H_2$ (NC1)		Met165	HN-O	3.11	H-bond
		Leu167	H-O	1.98	H-bond
		Arg188	N-O	1.85	H-bond
		Thr190	NH-O	1.92	H-bond
		His41, Glu166, Pro168, Gly170,			van der Waal bond
		Ala191, Gln192, Gln189,			van der Waal bond
		Asp187			halogen
Fav+$ZrTiO_4H_2$ (NC2)		Leu141	OH-O	1.84	H-bond
		Cys145	O-SG	3.59	H-bond
		His163	O-HE2	2.36	H-bond
		His164	NH-O	2.91	H-bond
		Glu166	OH-OE1	1.75	H-bond
		His41, Phe140, Asn142, Gly143,			van der Waal
		Met165, leu167, His172, Gln189			van der Waal

Ligand	Target Protein	Binding residue	Atoms	Bond length(Å)	Interaction
		Arg188			halogen
		Ser144			Unfavorable
Fav+$ZnTiO_4H_2$ (NC3)		Leu141	H-O	2.21	H-bond
		Ser144	H-OG	2.04	H-bond
		Cys145	O-SG	3.70	H-bond
		His163	O-HE2	2.33	H-bond
		Glu166	HN-OE1	1.92	H-bond
		His41, Phe140, Asn142, Gly143,			van der Waals
		His164,, Leu167, His172, Gln189			van der Waals
		Arg188			halogen
		Met165			Pi-Alkyl

Table S22 Interaction of Spike-ACE_2 protein residues with favipiravir, Fav+ $XTiO_4H_2$ nanocomplex.

Ligand	Target Protein	Binding residues	Atoms	Bond length(Å)	Interaction
Favipiravir	Spike-ACE2	Tyr279	NH-O	1.95	H-bond
		Pro289	H-O	1.95	H-bond
		Ile291	NH-N	2.22	H-bond
		Asn437	HD-O	2.30	H-bond
		Lys288, Met366, Phe428,			van der Waals
		Thr434, Phe438, Lys441			van der Waals
		Asn290,			halogen
Fav+Pt TiO_4H_2 (NC1)		Ile291	N-O	1.82	H-bond
		Ala413	NH-O	2.48	H-bond
		Tyr279, Pro289, Asn290, Met336			van der Waals
		Leu418, Phe428, Thr434, Glu435,			van der Waals
		Lys541			van der Waals
		His540			carbon-hydrogen bond
		Leu410			halogen
		Asn437			Unfavorable donar-donar
		Thr414			Pi-sigma
		Phe438			Pi-Pi stacked
		Pro415			pi-alkyl

Ligand	Target Protein	Binding residues	Atoms	Bond length(Å)	Interaction
Fav+Zr TiO_4H_2 (NC2)		Pro289	NH-O	1.78	H-bond
		Ile291	O-NH	1.84	H-bond
		Thr434	F-HG	2.47	H-bond
		Asn290, Phe428, Glu430, Asp431, Glu435, Phe438, Lys441			van der Waals
					Pi-alkyl
		Pro415			Pi-alkyl
Fav+Zn TiO_4H_2 (NC3)		Pro289	NH-O	1.68	H-bond
		Asn290	NH-N	2.23	H-bond
		Ile291	O-HN	1.78	H-bond
		Thr434	F-H	2.52	H-bond
		Phe428, Glu430, Asp431, Glu435, Phe438, Lys441,			van der Waals
					van der Waals
		Pro415			Pi-alkyl

Table S23 Physicochemical properties, lipophilicity, water solubility and drug-likeness of favipiravir and $XTiO_4H_2$ nanocomplexes.

Properties	Favipiravir	Fav+PtTiO2	Fav+ZrTiO2	Fav+ZnTiO2
Molecular weight (g/mol)	157.1	472.1	363.2	342.4
Num. heavy atoms	11.0	17.0	17.0	17.0
Num. rotatable bonds	1.0	0.0	0.0	0.0
Hydrogen bond acceptors	4.0	10.0	9.0	10.0
Hydrogen bond donors	2.0	5.0	4.0	5.0
Molar refractivity	32.9	46.3	45.1	46.3
TPSA(Å²)	88.8	127.5	127.9	127.5
Bioavailability Score	0.6	0.6	0.6	0.6
Log S(ESOL)	-0.8	-1.5	-0.7	-0.7
log Kp(cm/s)	-7.7	-10.7	-10.1	-9.9
Lipinski's RO5, violations	0.0	0.0	0.0	0.0
Log Po/w(iLOGP)	0.4	0.0	0.0	0.0
Log Po/w (XLOGP3)	-0.6	-2.1	-2.2	-2.1
Log P o/w (WLOGP)	-0.6	-2.4	-1.6	-2.4
Log P o/w (MLOGP)	-1.3	-4.9	-5.2	-4.9
Log P o/w (SILICOS-IT)	0.7	-4.3	-3.8	-5.1
Consensus Log Po/w	-0.3	-2.7	-2.6	-2.9

Table S24 Toxicity prediction of the favipiravir, Fav+$PtTiO_4H_2$, Fav+$ZrTiO_4H_2$, Fav+$ZnTiO_4H_2$ nanocomplexes using ProTox II.

Properties	**Favipiravir**	**Fav+$PtTiO_4H_2$**	**Fav+$ZrTiO_4H_2$**	**Fav+$ZnTiO_4H_2$**
Predicted LD_{50} (mg/kg)	1717	400	114	3000
Predicted toxicity class	4	4	3	5
Hepatotoxicity (prediction/ probability)	Inactive/ 0.66	Inactive/ 0.63	Inactive/ 0.63	Inactive/ 0.63
Carcinogenicity (prediction/ probability)	Active/0.53	Inactive/ 0.59	Inactive/ 0.58	Inactive/ 0.59
Immunotoxicity (prediction/ probability)	Inactive/ 0.99	Inactive/ 0.99	Inactive/ 0.97	Inactive/ 0.99
Mutagenicity (prediction/ probability)	Inactive/ 0.76	Inactive/ 0.99	Inactive/ 0.56	Inactive/ 0.56
Cytotoxicity (prediction/ probability)	Inactive/ 0.84	Inactive/ 0.56	Inactive/ 0.60	Inactive/ 0.60

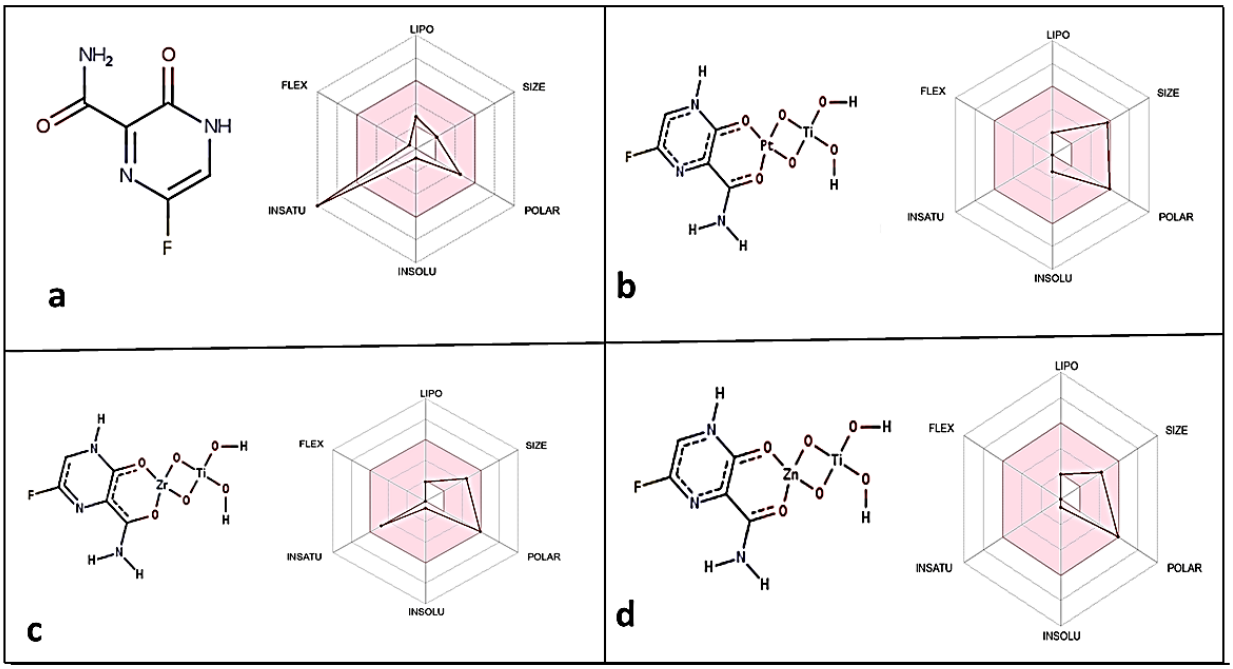

Figure S16 Bioavailability radar diagram of (a) favipiravir, (b) Fav+$PtTiO_4H_2$, (c) Fav+$ZrTiO_4H_2$, and (d) Fav+$ZnTiO_4H_2$ nanocomplexes.